# Control of the Deposition Ratio of $Bi_2Te_3$ and $Sb_2Te_3$ in a Vacuum Evaporator for fabrication of Peltier Elements

L. M. Gonçalves, J. G. Rocha, J. H. Correia and C. Couto
Industrial Electronics Department, University of Minho,
Campus de Azurem 4800-058 Guimaraes, Portugal.
Email L. M. Gonçalves: lgoncalves@dei.uminho.pt

***Abstract*— This article reports the main problem and the corresponding solution of the co-evaporation of $Bi_2Te_3$ and $Sb_2Te_3$ films for the fabrication of Peltier elements. This main problem consists in the control of the deposition rates of the two elements: Bi or Sb and Te, which have very different vapor pressures. The control of the deposition ratio was achieved by means of a PID controller, which permitted the fabrication of thin-film Peltier elements that produce a temperature gradient in the order of $2^{\circ}C$ between their hot and cold junctions, when measured at free air conditions.**

## I. Introduction

There are many industrial processes that use thin-film technology: optical coatings of filters and lenses, microelectronics, microsensors, etc. A simple way to deposit thin films is achieved by evaporation. The material to be deposited is heated until it reaches the vapor state. The substrate (optical filter or lens, for example) is placed above the material to be deposited. The atoms of the material that constitute the thin-film will then adhere to the substrate surface. In many cases, only the thickness of the deposited thin-film is important, so the control can be done in a simple way: the electrical power of the heater must be enough to start the evaporation and it must be switched off when the desired thickness is achieved.

For the fabrication of thin-film Peltier elements, instead of single element substances, they are used compounds [1]. Unfortunately, the deposition of compound substances like $Bi_2Te_3$ and $Sb_2Te_3$ is not as simple as the elementary substances described above. This phenomenon is described along this article, in its references and in related literature.

Commercial Peltier devices are usually fabricated on a transversal (cross-plane) configuration as is shown in figure 1. In theory, this configuration could be reduced for micro-device fabrication, but the conventional fabrication processes are not scalable to the micrometer range. Using a lateral (in-plane) configuration (figure 2), thin-film techniques can be used to scale down the thermoelectric coolers and generators to micro-device dimensions [2]. In the present work, planar thin-film technology will be used to fabricate such devices.

The Peltier element consists in $pn$ semiconductor junctions where the $n$-type semiconductor is the $Bi_2Te_3$ and the $p$-type semiconductor is the $Sb_2Te_3$. Tellurium alloys are well-established low-temperature thermoelectric materials and are

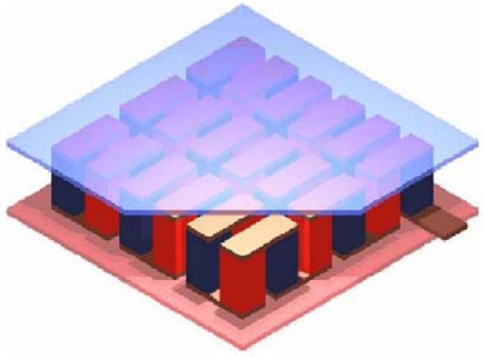

Fig. 1. Cross-plane (transversal) Peltier cooler.

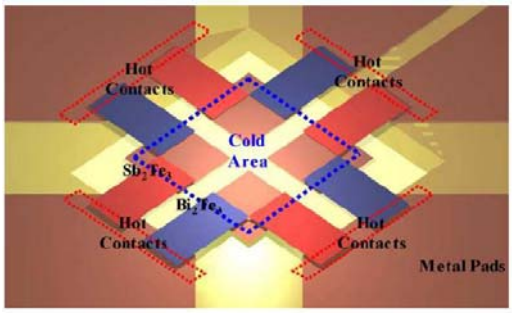


Fig. 2. In-plane (lateral) Peltier cooler.

widely employed in conventional thermoelectric generators and coolers [3]. Different deposition techniques can be used to obtain $Bi_2Te_3$ and $Sb_2Te_3$ thin-films. Thermal co-evaporation [4], co-sputtering [5], electrochemical deposition [6], metal-organic chemical vapor deposition [7] and flash evaporation [8] are some examples.

The objective of the work is to fabricate the $Bi_2Te_3/Sb_2Te_3$ junctions, from the Bi, Te and Sb elementary substances individually using a co-evaporation technique. In this case, both the thickness of the film and the evaporation rate of each element must be well controlled. In order to do that, we developed a control setup consisting on a digital PID controller,

1-4244-0497-5/06/$20.00 © 2006 IEEE

sensors and actuators.

The choice of the co-evaporation method is due mainly because it is inexpensive, simple and reliable, when compared to other techniques that need longer time periods to prepare the starting material or require more complicated and expensive deposition equipments.

The developed setup allowed the achievement of very promising results in the fabrication of planar thin-film Peltier elements.

## II. Thin-film co-evaporation

Bismuth, tellurium and antimony have large differences in their vapor pressures. These differences would result in a compositional gradient along the film thickness, when $Bi_2Te_3$ and $Sb_2Te_3$ films are directly evaporated from the compounds. This composition gradient effect is also reported in literature [9]. The problem of composition gradient can be overcome, though, by the use of co-evaporation [4], where Bi and Te are evaporated in a vacuum chamber, from two molybdenum boats, whose temperatures are independently controlled. A similar procedure was adopted for $Sb_2Te_3$ deposition from two independent Sb and Te sources.

Figure 3 shows a schematic diagram of the co-evaporation system used in the fabrication of the films. It consists in a

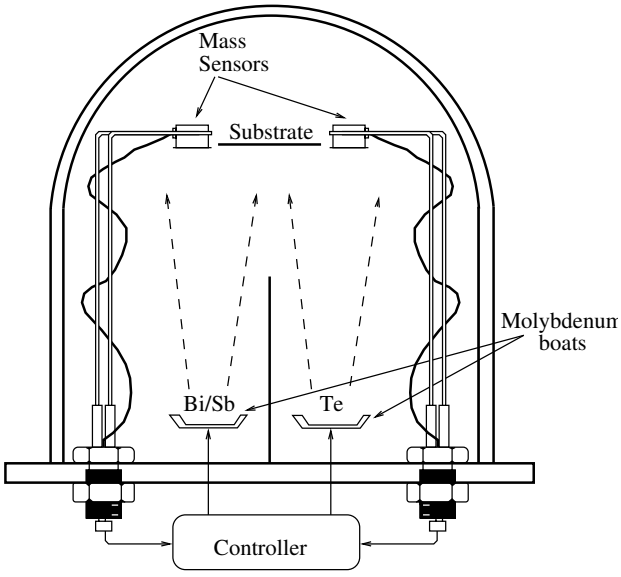


Fig. 3. Co-evaporation system.

vacuum chamber where the pressure reaches $10^{-6}\ mbar$. In its interior two evaporation boats are placed: the first one holds the Bi or the Sb samples and the second one holds the Te sample. The boats are separated by a metallic wall and are heated by means of an electric current ranging between $100\ A$ and $200\ A$, which is supplied by the controller. At the top of the chamber are placed the substrate where the deposition is made and two mass sensors. The objective of the metallic wall that separates the two boats is to avoid the deposition of the material of the left boat in the right sensor and vice-versa.

Table I shows the evaporation temperatures of the materials that were used in the fabrication of the Peltier elements, at the pressure of $10^{-6}\ mbar$. The Two sensors were used to

TABLE I
Temperature of evaporation of the materials at $10^{-6}\ mbar$ of pressure.

| Material | Temperature ($^oC$) |
|---|---|
| Bi | 410 |
| Sb | 345 |
| Te | 207 |

monitor the deposition rate of Bi/Sb and Te. Each rate was maintained at a fixed value, through independent control of the power applied to each molybdenum evaporation boat. The evaporation rate must be between $0.2\ nm/s$ and $0.4\ nm/s$ for good film properties.

## III. Control setup

Basically, the control of the evaporation rate is made by regulating the voltage and consequently the current that is applied to the boats. In order to implement this control, it is necessary to sense the deposited material, read the output of the sensors and act in the voltage applied to the boats. In the following subsections, these items will be described with great detail.

### A. Sensors

The sensor uses the resonant frequency of an exposed quartz crystal to sense the mass of deposited films attached to its surface. The presence of mass of the deposited film on the surface of the crystal decreases its resonant frequency. The relationship between the mass of the film and the frequency of the sensor crystal is given by [10]:

$$h = \left(\frac{N_Q d_Q}{\pi d_F Z f}\right) \arctan\left[Z \tan\left(\frac{\pi(f_Q - f}{f_Q}\right)\right], \qquad (1)$$

where the terms used in the equation are defined as:

$h$ - film thickness;

$N_Q$ - frequency constant for AT-cut quartz crystal ($1.668 \times 10^{13}\ Hz$.Å);

$d_Q$ - density of quartz ($2.648\ g.cm^{-3}$);

$d_F$ - density of film material;

$Z$ - Z-Factor of film material;

$f_Q$ - frequency of crystal prior to depositing any film on it;

$f$ - frequency of loaded crystal.

The Z-factor of the material can be calculated using the equation:

$$Z = \sqrt{\frac{d_Q S_Q}{d_F S_F}}, \qquad (2)$$

where the terms used in the equation are defined as:

$d_Q$ - density of quartz;

$S_Q$ - shear modulus of quartz ($2.947 \times 10^{11}\ g.cm^{-1}.s^{-2}$);

$d_F$ - density of film;

$S_F$ - shear modulus of film.

The contacts to the crystal are gold plated to ensure low resistance and avoid oxidation. Measuring the frequency of the

signal generated on the oscillator, the thickness is calculated each four seconds. The evaporation rate is obtained by the change of thickness. The crystal sensors are placed in such way that they receive exactly the same quantity of material that reaches the substrate. The crystal sensors are water cooled (around $20^oC$) to minimize the influence of temperature on oscillating frequency.

### B. Readout device

The readout circuit of the sensors is shown in figure 4. It consists basically in a series resonant crystal oscillator configuration and uses two cascaded inverters, which form an amplifier. Each inverter has a DC biasing resistor which biases

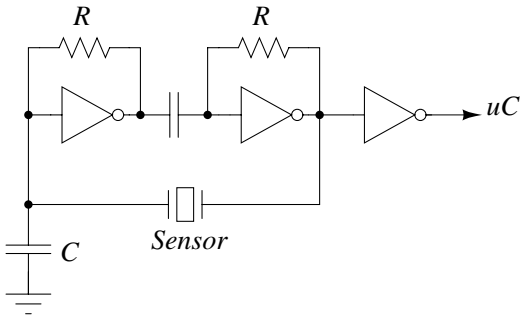


Fig. 4. Readout circuit of the mass sensors.

the inverter in the active region, i. e. halfway between the logic "1" and "0" states. In this region, the inverters act as high gain inverting amplifiers, introducing a phase shift of $180^o$ in the signal. The output of the circuit is connected to the microcontroller, which counts the number of pulses in a fixed time interval, obtaining in this way the mass of the material deposited in the sensor.

### C. Controller

The controller was implemented in a Philips Semiconductors P89C51RD2 microcontroller. Basically, it reads the output of the two sensor circuits and the phase of the power line and act in the switching angle of two triacs (one for each evaporation boat). Figure 5 shows the circuit that performs the phase detection of the power line voltage.

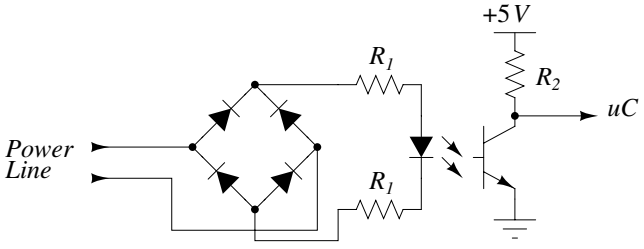


Fig. 5. Circuit that performs the phase detection of the power line voltage.

Figure 6 shows the triac switching circuit, where the switching angle is controlled by the microcontroller ($uC$) by means of an optocoupler. This circuit controls the voltage applied to the primary winding of a power transformer. The secondary of the transformer is directly connected to the evaporation boat.

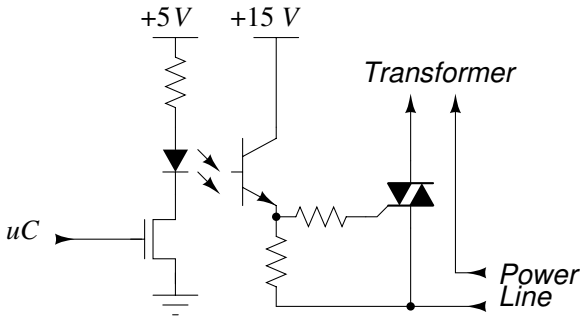


Fig. 6. Power switching circuit.

The algorithm used in the controller is a well-known PID. Nevertheless, the control of the evaporation ratio of a material has particular characteristics: below its vacuum evaporation temperature nothing happens and above this temperature, everything happens very quickly. In order to perform a good evaporation ratio control, the temperature inside the boats must be approximately equal to the evaporation temperature of the material, and change only some tenths of degree Celsius. In order to obtain this behavior, the output of the control algorithm was offsetted, i. e., without PID actions, the output of the controller will be the one that produce approximately the evaporation temperature of the material. With the introduction of this offset, the control algorithm worked fine, allowing the fabrication of the desired films.

Figure 7 shows a picture of the circuit.

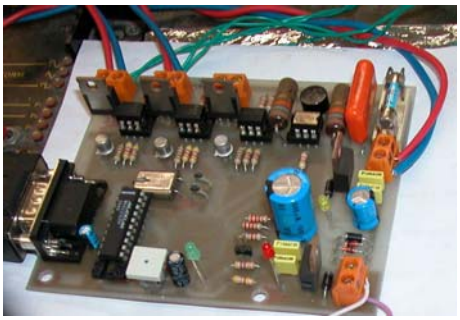

Fig. 7. Picture of the circuit.

### D. Actuators

The output of each circuit represented in figure 6 is connected to the primary winding of a transformer. The secondary winding of each transformer is directly connected to the respective molybdenum boat placed inside the vacuum chamber. Two transformers of 220 $V/6$ $V$, 1.2 $kVA$ were used, which permits a ranging of the current in the boats up to 200 $A$, depending on the switching angle of the triacs.

## IV. Experimental results

First of all, a test to the controller and the power electronics was performed. Figure 8 shows the waveform obtained at the evaporation boat terminals, for a switching angle of $100^o$.

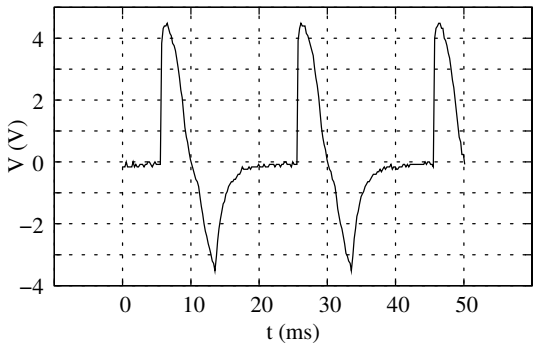


Fig. 8. Waveform at the evaporation boat terminals for a triac switching angle of $100^o$.

Figures 9 to 11 show the closed loop control performance of the system, for the deposition of the $Bi_2Te3$ film. The graphs for the deposition of $Sb_2Te_3$ are similar, except that the electrical power applied to the evaporation boat containing the Sb sample is a little bit smaller than the one of Bi. Figure 9 shows the evaporation rate of Te and Bi during the film fabrication. As it is possible to see, there are small oscillations around a mean value.

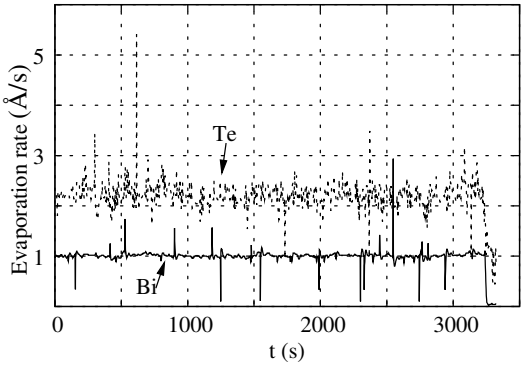


Fig. 9. Evaporation rate of Te and Bi during the fabrication of the $Bi_2Te_3$ film.

Figure 10 shows the film thickness deposited at each sensor as a function of time. As it can be seen (and calculated), the control response is highly linear for both materials. The Pearson product moment correlation coefficients are 0.999975 and 0,999977 respectively, i. e., very close to 1.

Figure 11 shows the electrical power supplied to each evaporation boat. From figures 9 to 11 referred above, it is possible to conclude that the controller is suitable to control with precision the evaporation ratio and the thickness of a co-evaporation process.

Figure 12 shows a picture of the fabricated device, which consists in four pairs of Peltier junctions. Each thermoelectric

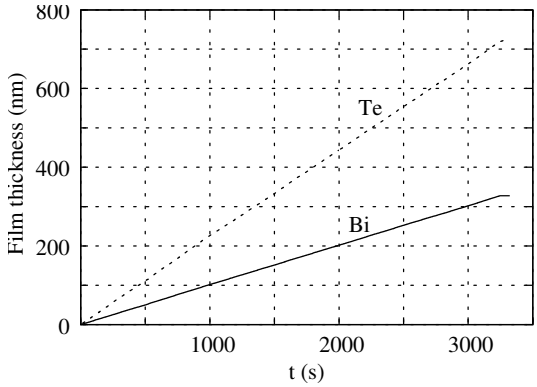


Fig. 10. Mass of Bi and Te deposited at each sensor as a function of time.

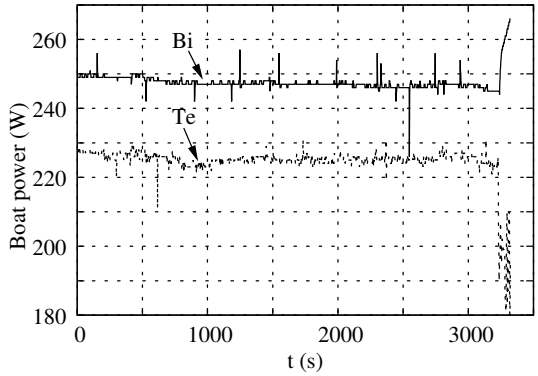


Fig. 11. Electrical power supplied to each evaporation boat.

leg has 2.3 $\mu m$ of thickness and the metal contacts have a thickness of 0.5 $\mu m$.

Figure 13 shows a cross-section of an homogeneous $Bi_2Te_3$ film with 700 $nm$ of thickness, fabricated in a previous experiment.

Table II shows the composition of the fabricated films, obtained by energy dispersive X-ray spectroscopy (EDX), and their respective Seebeck coefficients. Te and Bi/Sb content

TABLE II

Percentage of atoms obtained for each film and respective Seebeck coefficient.

| Material | Bi/Sb (%) (%) | Te (%) (%) | Seebeck $\mu V/^oC$ |
|---|---|---|---|
| $Bi_2Te_3$ | 39.83 | 60.17 | -189 |
| $Sb_2Te_3$ | 41.49 | 58.51 | 140 |

shows that the composition of both types of films is close to stoichiometry. An X-ray diffraction (XRD) analysis was also performed. That analysis revealed that the structure of the films is polycrystalline. The Seebeck coefficients were measured by connecting one side of the film to a heated metal block at a fixed temperature and the other side to a heat sink at room temperature. The voltage generated in these known conditions was then measured.

Figure 14 shows a thermal image of one of the fabricated Peltier elements, with an applied electric current of 5 $mA$.

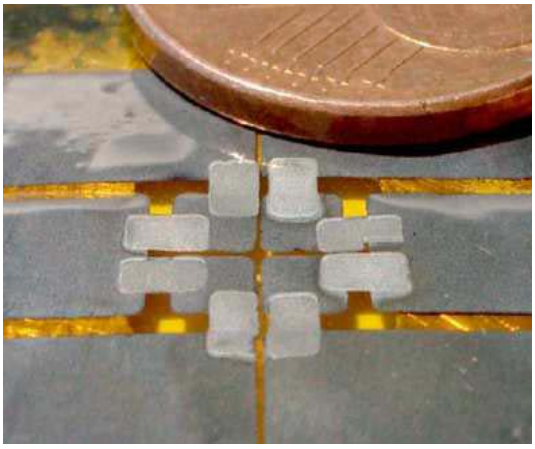

Fig. 12. Picture of the fabricated device.

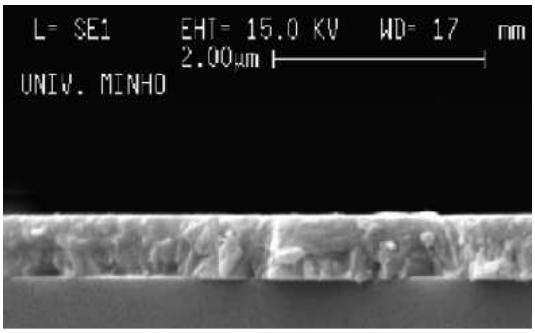


Fig. 13. SEM photograph of a homogeneous $n$-type 700 $nm$ thick $Bi_2Te_3$ film.

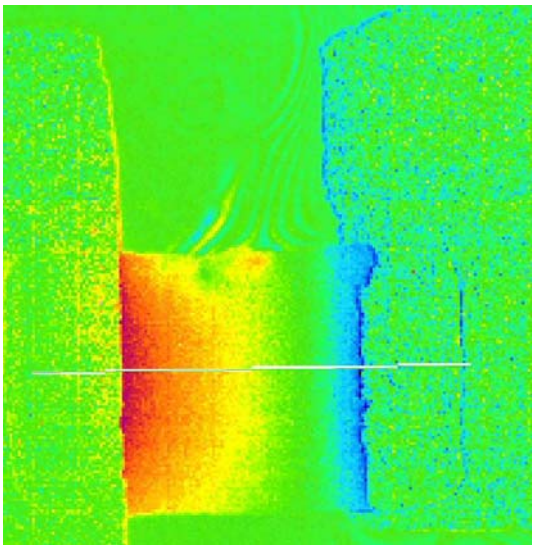

Fig. 14. Thermal image of the Peltier element.

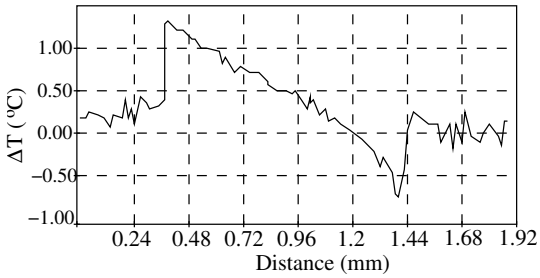


Fig. 15. Mapping of the temperatures along the line of figure 14.

Figure 15 shows a graph of temperature gradient versus distance, obtained along the line drawn in figure 14. The obtained temperature gradient was close to $2^oC$. This test was performed in a natural convection (still air) environment, resulting in a surface temperature map of the device as represented in figure 14.

## V. Conclusions

Peltier elements formed by junctions of $Bi_2Te_3$ and $Sb_2Te_3$ were fabricated using a co-evaporation technique. This technique is advantageous relatively to other possible ones because it is inexpensive, simple and reliable. The main difficulty of the co-evaporation consists in the control of the deposition rates of the two materials, which must be proportional between them in order to obtain a composition with the desired properties. The control of the evaporation rate was made by using a PID controller, which revealed very efficient. As result, thin-films of Peltier elements were obtained and it was reached the difference of temperatures between hot and cold junctions in the order of $2^oC$.

## References

[1] L. M. Gonçalves, C. Couto, P. Alpuim, D. M. Rowe and J. H. Correia, *Thermoelectric microstructures of $Bi_2Te_3/Sb_2Te_3$ for a self-calibrated micro-pyrometer*, Sensors and Actuators A (2006), article in press.

[2] G. Min and D. M. Rowe, *Cooling performance of integrated thermoelectric micro-cooler*, Solid-State Electron. 43 (1999) 923-929.

[3] D.M. Rowe, *CRC Handbook of Thermoelectrics*, CRC Press, 1995.

[4] H. Zou, D.M. Rowe and S.G.K. Williams, *Peltier effect in a co-evaporated $Sb_2Te_3$(p)-$Bi_2Te_3$(n) thin-film thermocouple*, Thin Solid Films 408 (2002) 270.

[5] H. Böttner, J. Nurnus, A. Gavrikov, G. Kühner, M. Jägle, C. Künzel, D. Eberhard, G. Plescher, A. Schubert and K. H. Schlereth, *New thermoelectric components using microsystem technologies*, J. Microelectromech. Syst. 3 (2004) 414.

[6] J. R. Lim, G. J. Snyder, C. K. Huang, J. A. Herman, M. A. Ryanand and J. P. Fleurial, *Thermoelectric micro-device fabrication process and evaluation at the jet propulsion laboratory*, 21st International Conference on Thermoelectronics, Long Beach, U.S.A., August 25 29 (2002) 535-539.

[7] A. Giani, A. Boulouz, F. Pascal-Delannoy, A. Foucaran, E. Charles and A. Boyer, *Growth of $Bi_2Te_3$ and $Sb_2Te_3$ thin-films by MOCVD*, Mater. Sci. Eng. B 64 (1999) 19-24.

[8] A. Foucaran, A. Sackda, A. Giani, F. Pascal-Delannoy and A. Boyer, *Flash evaporated layers of ($Bi_2Te_3$ $Bi_2Se_3$)(n) and ($Bi_2Te_3$ $Sb_2Te_3$)(p)*, Mater. Sci. Eng. B 52 (1998) 154-161.

[9] L. W. da Silva and M. Kaviany, *Miniaturized thermoelectric cooler*, ASME International Mechanical Engineering Congress and Exposition, New Orleans, U.S.A., November 17 22 (2002) 1-15.

[10] C. Lu and O. Lewis, *Investigation of film-thickness determination by oscillating quartz resonators with large mass load*, J. Appl. Phys. 43 (1972) 4385.